

148.
DETAILED MEASUREMENTS OF THE H β LINE
SHAPE IN A TRANSIENT PLASMA USING A FIBER OPTICS SLIT SYSTEM

G. H. Stickford, Jr.

May 1, 1972

(NASA-CR-126550) DETAILED MEASUREMENTS OF
THE H BETA LINE SHAPE IN A TRANSIENT PLASMA
USING A FIBER OPTICS SLIT SYSTEM G.H.
Stickford, Jr. (Jet Propulsion Lab.) 1 May
1972 12 p

N72-24710

Unclas
CSCL 20F G3/23 28482

Backup Document for AIAA Synoptic Scheduled for
Publication in the AIAA Journal, October 1972

Jet Propulsion Laboratory
California Institute of Technology
4800 Oak Grove Drive
Pasadena, California 91103

Details of illustrations in
this document may be better
studied on microfiche

DETAILED MEASUREMENTS OF THE H β LINE SHAPE IN A
TRANSIENT PLASMA USING A FIBER OPTICS SLIT SYSTEM** +

G. H. Stickford, Jr.
Jet Propulsion Laboratory
Pasadena, California

Abstract

Through the use of fiber optics, a series of very narrow slits have been constructed and placed at the exit plane of a spectrograph. Plasma radiation which is dispersed by the spectrograph is incident on the slits and is transmitted to separate phototubes via the quartz fibers. With this technique, time resolved measurements of the spectral shape of the hydrogen H β line have been made and used to determine the electron density of a transient plasma. Data obtained in a shock tube indicated that the thermodynamic conditions behind the reflected shock in a mixture of 20% H $_2$ - 80% He, at incident shock speeds of 12 to 14 km/sec and pressures of 66.6 to 133.3 N/m 2 (0.5 to 1.0 mm Hg), correspond to theoretically predicted conditions. Immediately behind the incident shock at speeds of 17 to 24 km/sec the data indicate that the plasma reached equilibrium then demonstrated a drop in intensity which has been attributed to radiative cooling.

I. Introduction

In conducting experimental studies with high temperature plasmas it is often more difficult to specify the thermodynamic and thermochemical conditions of the plasma than to make the necessary experimental measurements. In general, one is required to determine the temperature, the pressure or bulk density, and the electron density. If the plasma is not in local thermodynamic equilibrium, one must also specify the heavy particle temperature. In transient plasmas, with which this report deals, the problem is further complicated by the fact that the measurements must all be made over a time period of a few microseconds.

There are many standard methods of measuring plasma properties. A good summary is given in Ref. 1. These techniques rely on the specific characteristics of the radiative spectra emitted by the plasma. By carefully monitoring the emitted spectra it is possible to determine all the required properties needed to completely specify the thermodynamic and thermochemical conditions of the plasma.

This paper describes a simple new technique for making electron density measurements in transient plasmas. One can also obtain the temperature if the pressure or density is known. Results are presented which demonstrate the effectiveness and the overall accuracy of the technique.

II. Determination of Hydrogen H β Line Shape

Computation of Shape

The presence of electrons and ions in a plasma have a large effect on the discrete or line emission from bound-bound atomic transitions. Stark broadening of the lines, due to electron and ion collisions, is the dominant broadening mechanism in singly ionized plasmas (10,000 to 20,000°K) and is strongly dependent on the electron density and nearly independent of the temperature. Thus, it is an excellent monitor of the electron density.

Stark broadened line profiles for hydrogen have been computed by Griem, Kolb, and Shen⁽²⁾ and are tabulated by Griem⁽¹⁾. An estimate of the theoretical accuracy is placed at 15%. However, a later experiment by Hill and Gerardo⁽³⁾ suggest that the profile for the H β line may be much better. Their measured profiles agreed to within $\pm 2\%$ of the calculated profiles.

The H β profile is probably the best known spectral indicator of the electron density. For this reason, together with the fact that this line is located in a favorable position of the spectrum, it was decided to concentrate on making time resolved H β profile measurements. Furthermore, if one at the same time obtains absolute intensity measurements of the profile, it is possible to deduce the temperature of the plasma as well.

The procedure used in this study is an iterative one where the line profile is experimentally measured and the theoretical profile is computed assuming a temperature and electron density. The electron density is then varied until the calculated line shape matches the measured shape. The matching criteria used is a least squares fit between the measured points and the computed points.

Following Griem⁽¹⁾, the line shape is given by

$$I_{\lambda} = \frac{S(\alpha)}{F_0} \quad (1)$$

where

$$F_0 = \frac{2.61e}{4\pi\epsilon_0} (N_e)^{2/3} = 1.253 \times 10^{-9} (N_e)^{2/3}$$

*This work was prepared under contract No. NAS7-100 sponsored by the National Aeronautics and Space Administration.

+This is a revision of AIAA paper 72-106.

is the field strength for single charged ions, N_e is the electron density in cm^{-3} . For an isothermal plasma of depth X , in cm, the spectrally emitted line intensity is

$$I_\lambda(X) = B_\lambda (1 - e^{-S I_\lambda X}) \quad (2)$$

where S is the line strength, in consistent units is

$$S = 0.8834 \times 10^{-4} \lambda_o^2 g_1 f_{lu} \left(\frac{N_a}{Q(T)} \right)$$

$$\times \left[e^{-E_u/kT} \left(e^{hc/\lambda_o kT} - 1 \right) \right]$$

The line center wave length, λ_o , is in cm, the atom number density, N_a , is in cm^{-3} ; g_1 is the lower level statistical weight, f_{lu} is the absorption oscillator strength, $Q(T)$ is the partition function, and E_u is the upper level energy.

The line shape parameter, $S(\alpha)$, is tabulated in Ref. 1 at 19 wave length points from the line center out to a point where the intensity drops to about 1/20 of the line center intensity. Shapes are given for four temperatures (5,000, 10,000, 20,000, 40,000°K) and four electron densities (10^{14} , 10^{15} , 10^{16} , 10^{17}cm^{-3}). For intermediate values, an interpolation scheme was used whereby the table was interpolated linearly between the listed temperatures, and logarithmically between listed electron densities.

The line shape calculations to be presented account for reabsorption although this effect is never greater than 10% of the emitted intensity. Emission from other sources, such as the continuum processes and the extended wings of other lines, was neglected since they contribute less than 1% to the line intensity.

Description of Line Shape Measurement Technique

Spectral measurements of the H β profile in plasmas with electron densities of 10^{16} to 10^{17}1/cm^3 require a wavelength resolution of at least 2 to 3Å. This resolution was obtained by constructing the fiber optics slit system* shown in Fig. 1. The slit system consists of seven slits 0.2mm wide and spaced every 0.5mm as shown in Fig. 2b. The slits are filled with three rows of quartz fibers approximately 75mm dia. and 30cm long. The fibers from each slit are individually bundled and can be optically connected to separate phototubes. Thus, each phototube monitors the radiation incident on one of the seven slits, giving a spatial resolution of 0.5mm.

These slits were placed in the focal plane of a Jarrel Ash Model 75-000 Plane Grating Spectrograph (f/6.3, 0.75m focal length). The grating is blazed for 5000Å, is ruled to 1200 grooves/mm and has a reciprocal linear dispersion of approximately 9Å/mm (at 4861Å). The slit spacing is therefore

4.5Å, with each slit viewing a spectral band pass of 1.8Å.

Slit Function and Aperture Angle

The slit function for the fiber filled slits has been computed for several cases of fiber orientation within the slits. The details of the calculations are presented in Ref. 4. Due to the large half-width of the H β line relative to the slit-width, the slit function has a minor effect on the measured shape of the line. The slit function was accounted for by computing the effective shape of the line as would be seen through the fiber optic slit system using the theoretical slit function. Thus, the computed profiles to be presented include the slit function correction.

The exit f/number of the spectrograph is 6.3. In order to collect all the radiation coming from the spectrograph grating, the slits must have an aperture angle greater than

$$\theta = \tan^{-1} \frac{1}{2 \text{ f/number}} = 4.5 \text{ deg}$$

The effective aperture angle of the slits was measured by allowing a beam of parallel rays to fall on the slits. The transmitted intensity was monitored as the incident angle was varied. The intensity was found to drop to half its value as the angle was varied from 0 to 12 deg. Thus, the effective aperture angle is felt to be large enough to receive all rays incident on the slits at the spectrograph focal plane.

III. Experimental Procedure and Results

Test Setup

The experimental results to be discussed were obtained in the JPL Electric-Arc Driven Shock-Tube⁽⁵⁾. A schematic of the experimental setup is shown in Fig. 2. The shock velocity and the quality of the flow behind the shock was monitored over the two meters of tube just preceding the test port. The 15.2cm shock tube was 10cm long, the testport was located 8cm from the diaphragm. The spectrograph was positioned to view a small region of test gas through a quartz window. The volume of test gas viewed was small enough to insure good time resolution as the plasma flows past the test port.

In addition to the normal straight through configuration, the shock tube can be operated in a reflected shock mode by positioning an endplate several millimeters behind the test port. The spectrograph thus views the reflected shock region. With an optical stop placed on the endplate the length of test slug viewed could be varied.

The fiber optics slit system was located at the exit plane of the spectrograph. Seven RCA 1P28 phototubes were used to monitor the radiation

*The fiber optics slit system was constructed by the Mosaic Fabrications Division of Bendix Corporation, Sturbridge, Mass.

transmitted through the fiber bundles. The phototube power supply and amplifying circuitry are discussed in Ref. 6. The response time of the phototubes and attendant circuitry is normally 0.1 to 0.2 μsec , however, due to an error in the phototube circuits it was discovered that the response time for the measurements to be presented was approximately 1 μsec . This is still sufficient response time for the present experimental measurements.

Calibration

The calibration of the total system was accomplished by placing a known radiation source at the center of the shock tube. A spectral wavelength calibration was performed by locating known atomic lines produced by a Mercury-Cadmium gas lamp. The accuracy of the calibration was such that the spectral position of the exit slit could be specified to within 2\AA .

An absolute intensity calibration was performed using a carbon arc which has been shown to be a reliable radiation standard⁽⁷⁾. The intensity emitted by the arc was assumed to be equivalent to a 3806°K grey body with an emissivity of 0.97 as proposed by Null and Lozier⁽⁷⁾. The measured plasma intensity, in Watts/cm² - μm -Ster, is given by⁽⁴⁾

$$I_\lambda = \epsilon B_\lambda \left(\frac{E^M}{E^C} \right) \quad (3)$$

where ϵB_λ is the carbon arc emission and E^M and E^C are the phototube output voltages for the measurement and the calibration, respectively.

Results

The room temperature composition of the test gas was a commercial mixture of 20% H_2 and 80% He , supplied by the Matheson Co. Inc., Culamonga, Calif. A helium rich mixture was used to raise the resultant plasma temperature, at a given shock speed, thus, ensuring a large electron concentration. Profiles of the H_β line were measured behind the reflected shock wave at incident shock speeds of 12 to 14 km/sec, and behind the incident shock at speeds of 17 to 24 km/sec. This represents plasma conditions of temperature and electron density of 11,800 to 15,600°K, and $0.18 \times 10^{17}\text{cm}^{-3}$, respectively.

Shown in Fig. 3 is a representative example of a set of phototube output oscillograms. These results are from the reflected shock region for an initial pressure of 66.6 N/m^2 (0.5 mmHg) and an incident shock speed of 12.5 km/sec. The radiative intensity of each slit is displayed as a function of time along with the output of a wide band (visible) phototube viewing the test region. This phototube is generally used to indicate the arrival of the shock wave and the termination of the test at the arrival of the contact surface.

The spectral line intensity is seen to lag the radiation front detected by the wide band tube. This is at least partially due to the long response time of the 1P28 circuits. The traces do, however,

reach an equilibrium level and indicate a constant property test slug of at least 12 μsec . At an initial pressure of 33.3 N/m^2 (0.25 mmHg) the test times are approximately half as long, however, the traces still reach a plateau and remain constant for several μsec .

Behind the incident shock, data were obtained at shock velocities of 17 to 20 km/sec in 133.3 N/m^2 (1.0 mm Hg) and 21 to 24 km/sec in 33.3 N/m^2 . An example of this data is shown in Fig. 4 for an initial pressure of 133.3 N/m^2 and a shock velocity of 20.0 km/sec. The indicated test time is 10 to 12 μsec ; the intensity fall off will be discussed in the next section. The test times for the 33.3 N/m^2 data is estimated to be from 4 to 6 μsec . In this case, the "plateau" region was very short, on the order of 1 to 2 μsec .

IV. Discussion

In order to produce an equilibrium plasma in a test facility, it is necessary to first have sufficient time to establish thermodynamic equilibrium. This is particle time which is equivalent to $\frac{1}{2}$ to $\frac{1}{4}$ μsec laboratory time (time as indicated on the oscilloscope traces). Thus, at all conditions of the present experiment there is sufficient test time to allow the plasma to reach equilibrium within the test slug.

The second equilibrium criterion is that the electron population be large enough to insure that the number of excitation collisions (due primarily to electrons) is much larger than the number of de-excitation reactions due to spontaneous emission. The electron density required to maintain equilibrium at the temperatures of this experiment is $0.6 \times 10^{16} \text{ cm}^{-3}$. The electron densities range from 4 to 10 times greater than this minimum value for the data to be presented.

It is, therefore, concluded that for the present experimental conditions the plasma test slug should reach equilibrium within one microsecond after the passage of the shock wave, and to remain in equilibrium throughout the test slug. The plasma properties behind the incident shock and the reflected shock should correspond to the conditions predicted by the conservation equations and equilibrium thermodynamics.

Presented in Figs. 5 through 7 are the results of the H_β line intensity distribution measurements obtained for 12 shock tube runs. Fig. 5 presents reflected shock data and Figs. 6 and 7 are incident shock data. In each case the data are compared with the computed line intensity using the equilibrium plasma conditions corresponding to the measured shock speed and initial pressure of the run (the solid line), as computed using the JPL thermochemistry computer program.⁽⁸⁾

The dashed curves are least squares fit profiles which were determined by varying the electron density until the profile best matched the measured intensity. To do this required that the calculated profiles first be normalized to pass through the measured points. The normalization factor was chosen such that the average deviation of the calculated profile from the measured points was

zero. The electron density was then varied a few percent, a new profile calculated and compared with the measured points. This process was repeated until the sum of the squares of the average deviation was minimized. The final profile gave the measured electron density corresponding to the measured profile.

Without an additional experimental measurement it is impossible to infer any other independent plasma property from these measurements. Since the overall magnitude of the line intensity is dependent on both the temperature and the atom number density, one must specify one of these in order to determine the other. It is observed, however, that the line intensity varies with the 10th or 12th power of temperature in this range of temperatures. Therefore, a temperature variation of 2 or 3% will cause the intensity to vary 20 to 40%. On the other hand, the intensity varies directly with the density. A 2 or 3% density variation will only cause a 2 or 3% intensity variation. Since the measured intensity is generally within 20% of the computed intensity, it is possible to deduce from the data that the plasma temperature is within 5% of the computed temperature for all the runs examined, assuming the density is reasonably close to the predicted value.

Presented in Table 1 is a summary of 14 shock tube runs. The last column is a ratio of the best-fit measured electron density to the computed equilibrium electron density. In general, the electron density is within 20% of the computed value and on the average is about 10% low. In all cases, the data represent the measured intensity immediately behind the shock. Some runs experienced a decrease in measured intensity through the test slug. It is felt that this drop in intensity represents a loss in energy due to gas radiation.

The fact that radiative cooling is an important phenomenon behind the incident shock can be demonstrated by a closer examination of run 288. In this case the radiative flux is high and the test time is long so that the effect of cooling is emphasized. Looking back at the phototube outputs from run 288, shown in Fig. 9, it can be seen that the intensity rises to a peak level within $1\frac{1}{2}$ μ sec, then decreases slowly for 8 to 10 μ sec until the arrival of the contact surface. The line shape was measured just prior to the arrival of the contact surface and the results are presented in Fig. 7a along with the shape measured just behind the shock. The line intensity is over 50% lower than the equilibrium line intensity.

In order to determine the thermodynamic conditions corresponding to this new line shape, the least squares fit technique was again used. In this case both the temperature and electron density were varied until the computed line shape fit the experimental measurements. To do this required an assumption regarding the process by which the gas went from one point to the other. To simplify the analysis, two limiting cases were used: flow at constant density (corresponding to hypersonic cooling) and flow at constant pressure (corresponding to incompressible cooling).

In each case the pressure or density was held constant at the equilibrium value behind the shock and the temperature and electron density was varied to determine the best-fit profile. The results are shown in Table 2.

The measured electron density in column 2 is that obtained from the best-fit profile; the equilibrium electron density corresponds to the temperature in column 1 and the equilibrium density or pressure behind the shock. The indicated temperature reduction is something between 10 and 20% depending on the flow process. Comparing the measured and equilibrium density it is apparent that the final thermodynamic state corresponds very nearly to an equilibrium condition. Thus, the flow seems to be changing conditions while remaining in equilibrium. This is consistent with a cooling phenomenon as opposed to a nonequilibrium phenomenon, such as de-excitation due to radiative decay.

The importance of radiative cooling at these conditions is further demonstrated by comparing the radiative flux emitted by the test slug to the energy convected through the shock wave into the test slug. This ratio, called the radiative cooling parameter, Γ , is

$$\Gamma = \frac{\text{Frad}}{\frac{1}{2} \rho_1 V_s^2 A} \quad (7)$$

where Frad is the isothermal radiative flux emitted by the test slug, ρ_1 is the density before the shock, V_s the shock velocity, and A is the frontal area of the test slug. Radiative cooling is important whenever this parameter is near 0.1 or is larger. Shown in Fig. 8 is Γ computed for the present experimental conditions of the incident shock cases. All the runs above 20 km/sec will be greatly affected by radiative cooling. In fact, on several of the 18 km/sec runs, initial pressure 133.3 N/m² (1.0 mm Hg), a small amount of cooling was noticed.

V. Conclusions

Using a fiber optics slit system to obtain detailed spectral resolution, the H β line intensity profile has been measured in the shock tube for several different plasma conditions. In all but one case, the measured intensity agreed to within 20 to 50% of the computed intensity using equilibrium shock tube thermodynamic conditions. In terms of plasma conditions, the temperature was found to be within a few percent of the predicted temperature, and the electron density within 10 to 20% of the predicted electron density.

Radiative cooling was found to be an important process behind the incident shock at shock speeds of 20 km/sec and above. For one run the measured temperature dropped 10 to 20% through the test slug. Since the measured electron density indicated that thermodynamic equilibrium existed throughout the test slug, it was concluded that radiative cooling was responsible for the change in flow properties. A calculation of the radiative cooling parameter verified the importance of cooling at these conditions.

References

1. Griem, H. R., Plasma Spectroscopy, McGraw-Hill, Inc. (1964).
2. Griem, H. R., Kolb, A. C., Shen, K. Y., "Stark Broadening of Hydrogen Lines in a Plasma," Phys. Rev., Vol. 116, pp. 4 (1959).
3. Hill, R. A., and Gerardo, J. B., "Stark Broadening of H β , H γ , and H δ : An Experimental Study," Phys. Rev., Vol. 162, pp. 45 (1967).
4. Stickford, Jr., G. H., "A Fiber Optics Slit System Used for Time Resolved Diagnostics in a Transient Plasma," TM 33-492, Jet Propulsion Laboratory, Pasadena, Calif., 1971.
5. Menard, W. A., "A Higher Performance Electric-Arc-Driven Shock Tube," Quarterly Technical Review, Vol. 1, pp. 17, Jet Propulsion Laboratory, Pasadena, Calif., 1971.
6. Menard, W. A., Thomas, G. M., "Radiation Measurement Techniques," TR 32-975, Jet Propulsion Laboratory, Pasadena, Calif., 1966.
7. Null, M. R., and Lozier, W. W., "The Carbon Arc as a Radiation Standard," Temperature. Its Measurement and Control in Science and Industry, Vol. III, part 1, Basic Concepts, Standards, and Methods, pp. 551, Reinhold Publishing Corp, Chapman & Hall, Ltd., London.
8. Horton, T. E., and Menard, W. A., "A Program for Computing Shock Tube Gasdynamic Properties," TR 32-1350, Jet Propulsion Laboratory, Pasadena, Calif., 1969.
9. Goulard, R., "The Radiative Transfer Problem in Detached Shock Layers," AIAA Conference on Physics of Entry into Planetary Atmospheres, Paper No. 63-952 (1963).

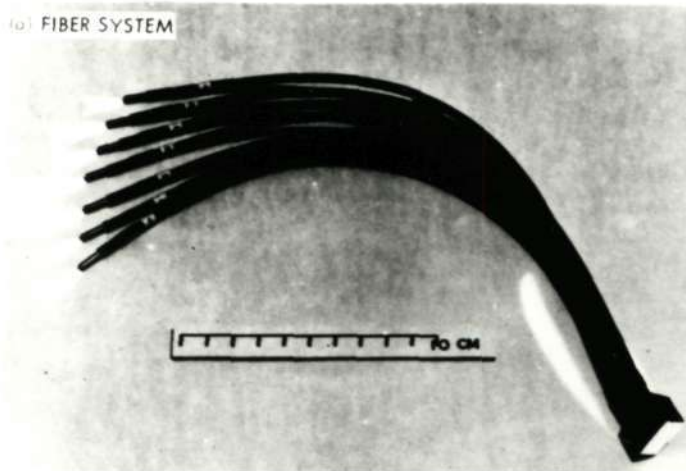
Table 1. Summary of shock tube runs

RUN No.	CONFIG.	P ₁ , N/m ² (mm hg)	V _s , km/s	T, K	Ne/Ne ideal	RMS Error
245	RS	33.3 (0.25)	14.0	13,825	0.992	3.9 %
252	RS	33.3 (0.25)	12.0	12,265	0.935	6.2
253	RS	33.3 (0.25)	12.5	12,610	0.790	10.5
257	RS	66.6 (0.50)	11.0	12,050	0.827	17.2
259	RS	66.6 (0.50)	12.9	13,425	0.881	19.8
283	IS	133.3 (1.0)	17.0	11,870	1.138	9.3
284	IS	133.3 (1.0)	18.05	12,540	0.935	5.0
285	IS	133.3 (1.0)	18.8	13,000	0.842	5.7
286	IS	133.3 (1.0)	18.3	12,690	1.013	5.0
287	IS	133.3 (1.0)	18.3	12,690	0.841	3.0
288	IS	133.3 (1.0)	20.0	13,710	0.779	6.2
290	IS	33.3 (0.25)	21.8	13,690	1.19	6.6
291	IS	33.3 (0.25)	21.4	13,460	0.947	8.8
292	IS	33.3 (0.25)	24.4	15,630	0.880	7.0
RS = REFLECTED SHOCK IS = INCIDENT SHOCK						

Table 2. Theoretical and measured conditions behind the incident shock,
V_s = 20.0 km/s, P₁ = 133.3 N/m²

Conditions	T, K	Measured Ne, 1/cm ³	Equilibrium Ne, 1/cm ³	Temperature reduction, %
Theoretical equilibrium conditions behind incident shock	13,710	—	0.465 × 10 ¹⁷	—
Measured electron density immediately behind incident shock	—	0.362 × 10 ¹⁷	—	—
Measured conditions 20 cm behind incident shock, assuming constant density flow	12,463	0.275 × 10 ¹⁷	0.288 × 10 ¹⁷	11.0
Measured conditions 20 cm behind incident shock, assuming constant pressure flow	11,677	0.275 × 10 ¹⁷	0.270 × 10 ¹⁷	17.5

(a) FIBER SYSTEM



(b) FIBER-FILLED SLIT

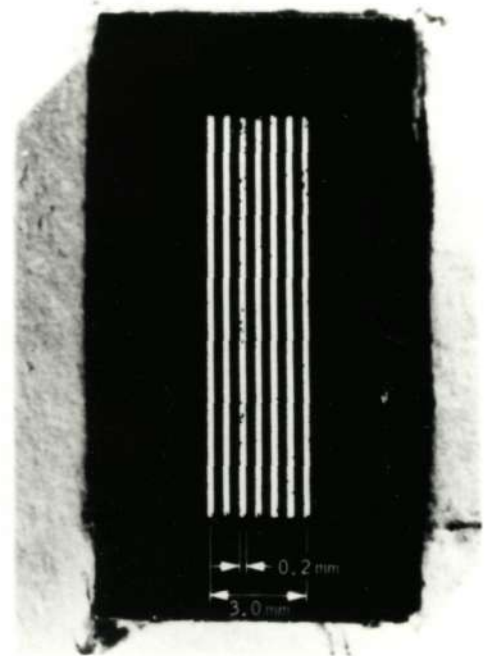


Fig. 1. Photograph of fiber optics slit system

Reproduced from
best available copy.

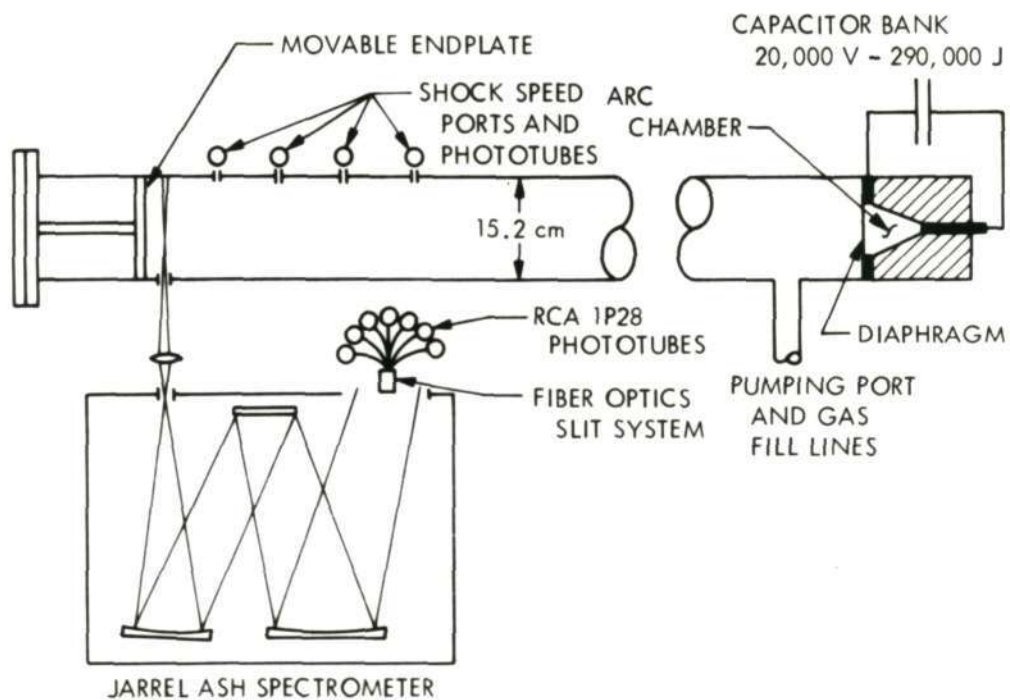


Fig. 2. Schematic of experimental setup showing JPL 15-cm arc-driven shock tube

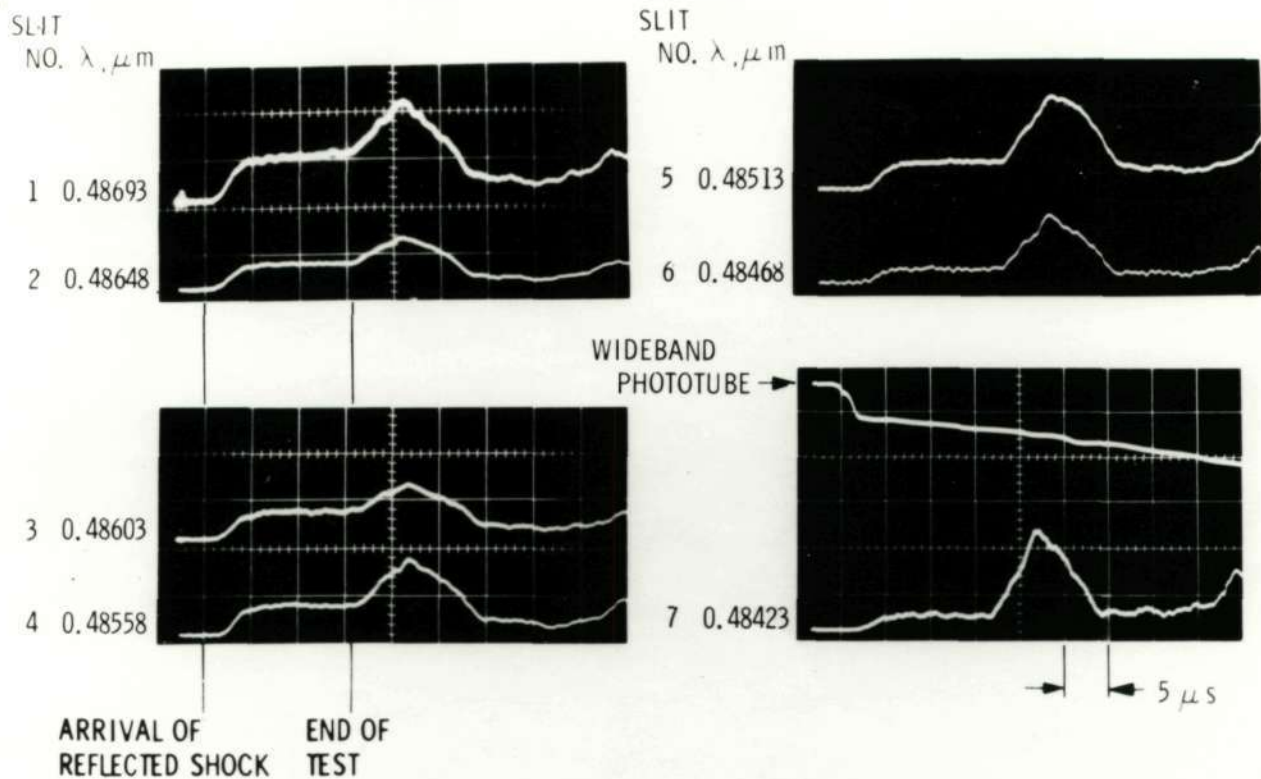


Fig. 3. Oscillograms of H β spectral intensity measurements, run 257,
 $P_1 = 66.6 \text{ N/m}^2$, $V_s = 12.5 \text{ km/s}$

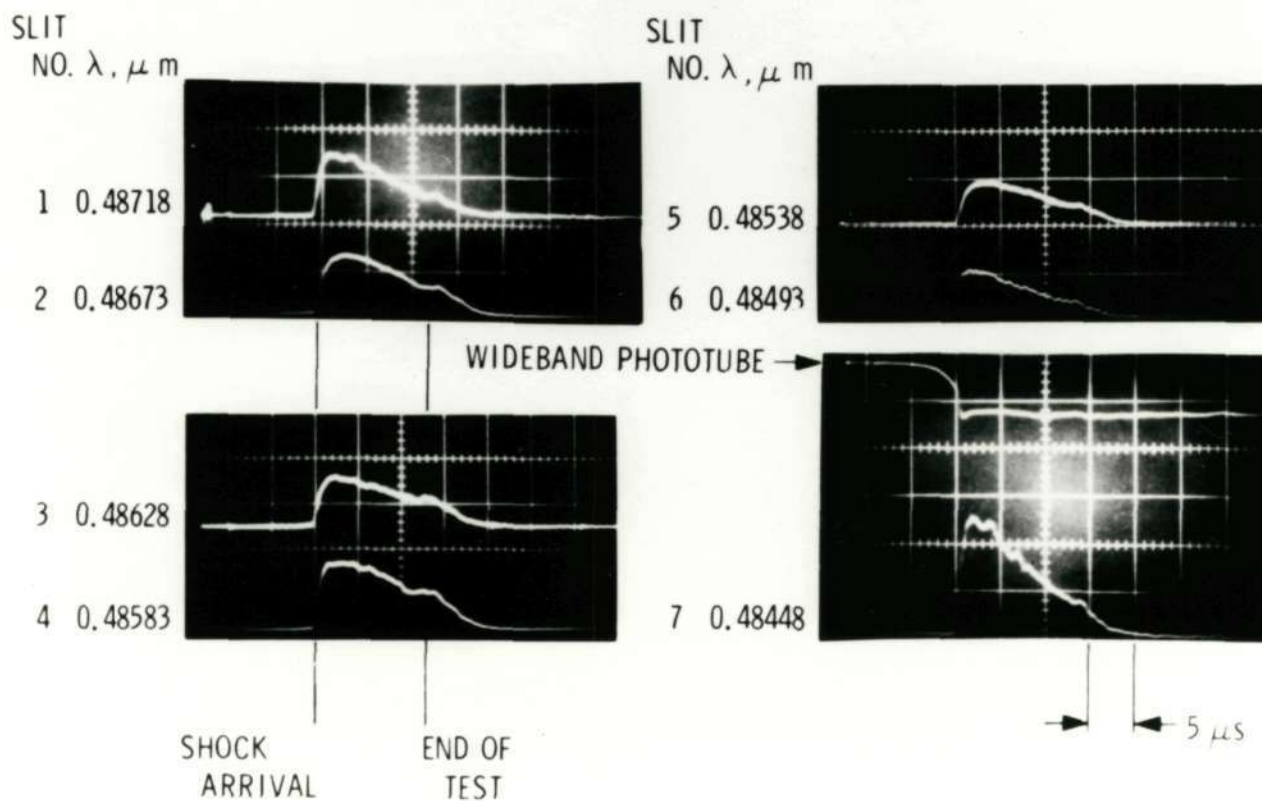


Fig. 4. Oscillograms of H β spectral intensity measurements, run 280,
 $P_1 = 135.3 \text{ N/m}^2$, $V_s = 20.0 \text{ km/s}$

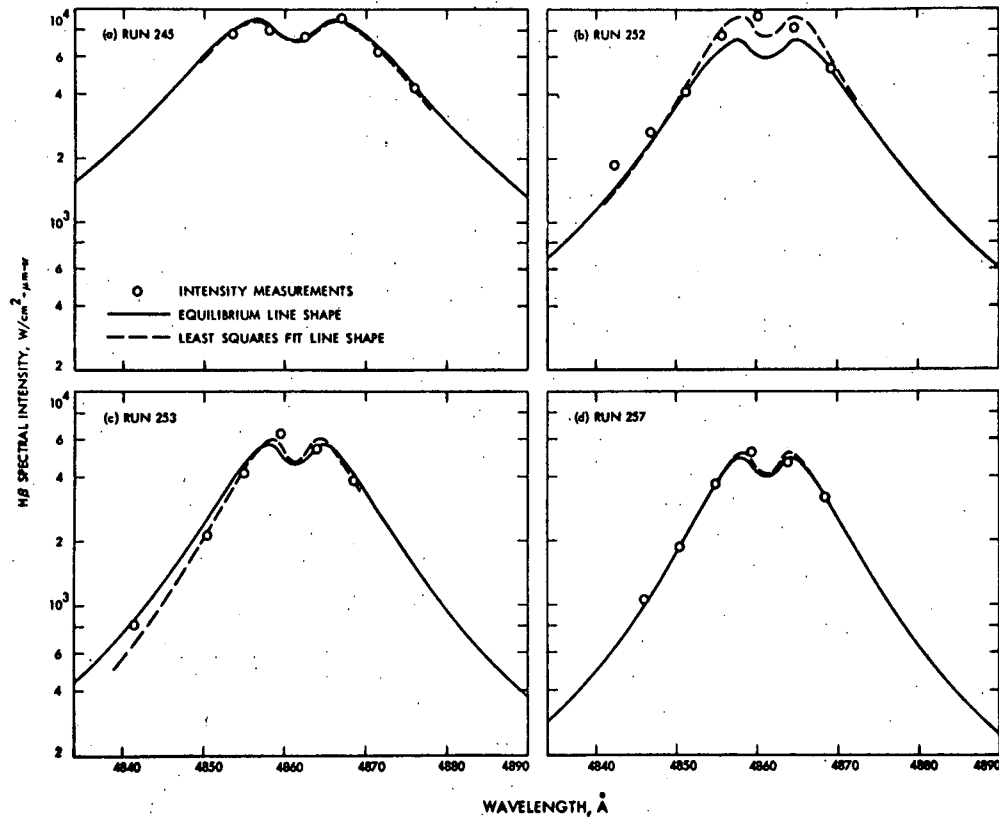


Fig. 5. H β spectral intensity data compared with the theoretical profile, reflected shock case

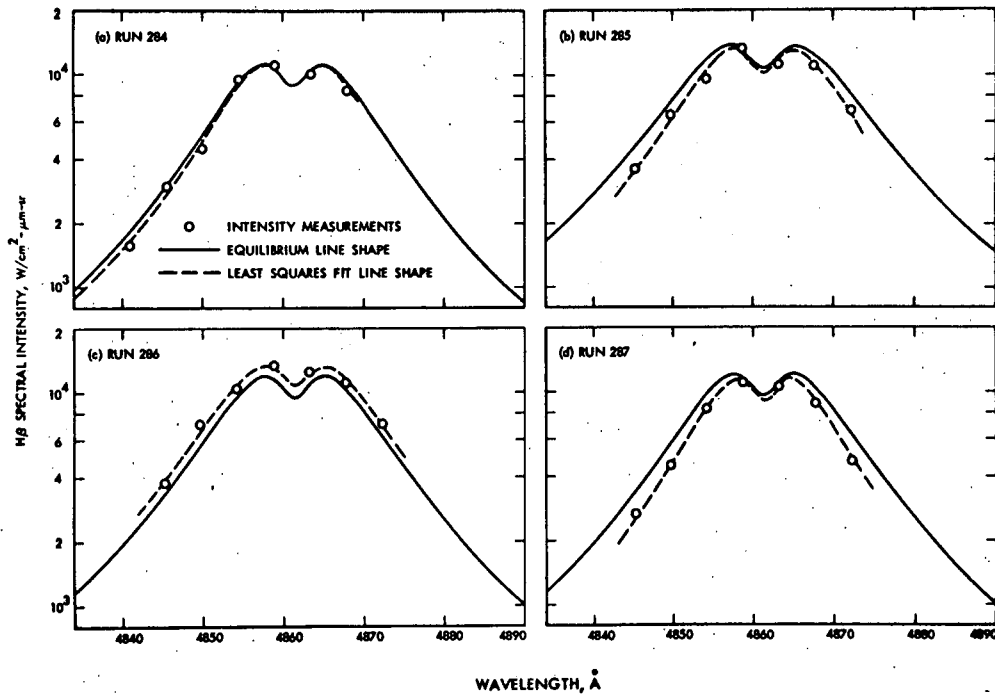


Fig. 6. H β spectral intensity data compared with the theoretical profile, incident shock case (runs 284-287)

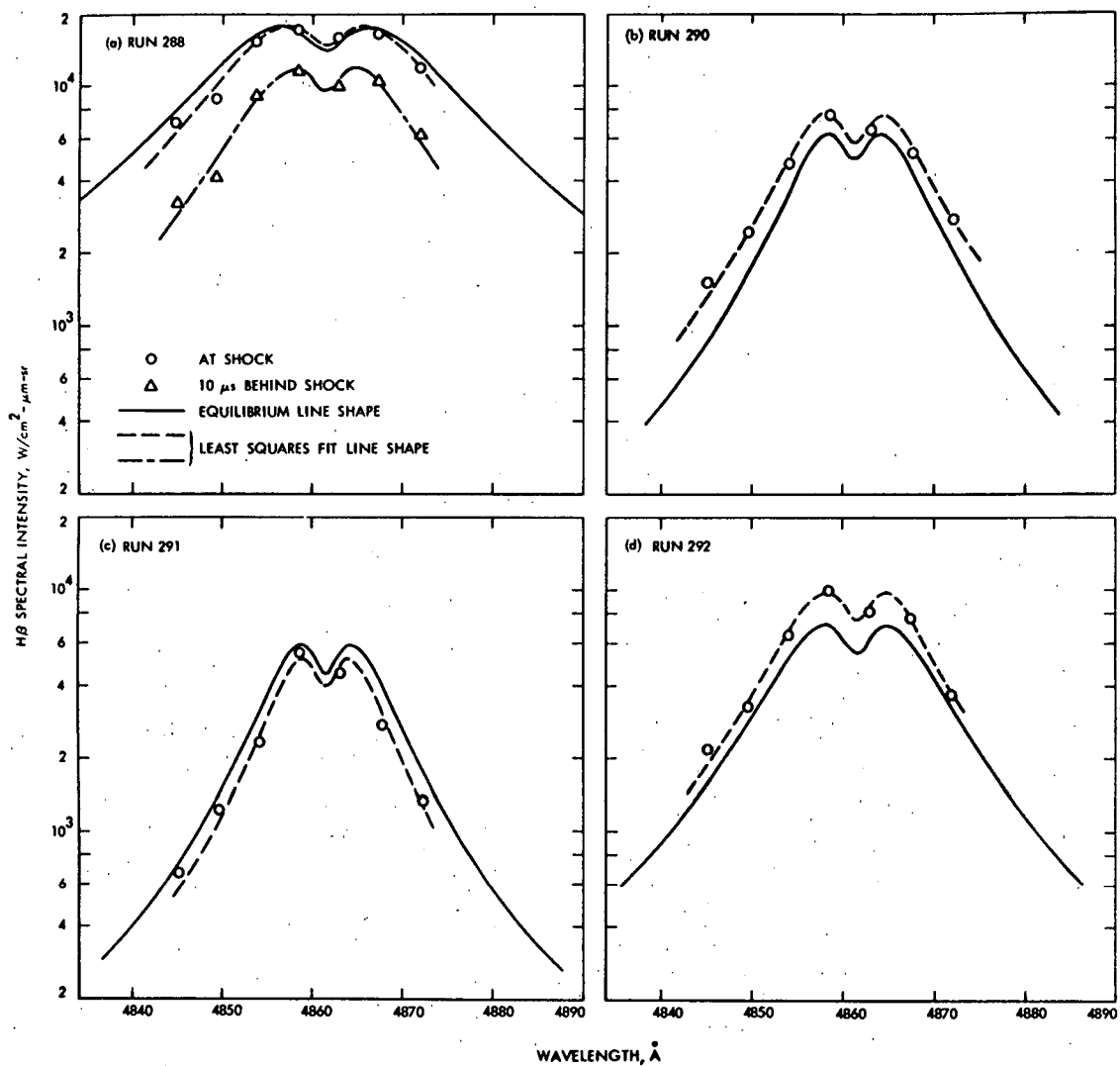


Fig. 7. H β spectral intensity data compared with the theoretical profile, incident shock case (runs 288, 291, 292, 293)

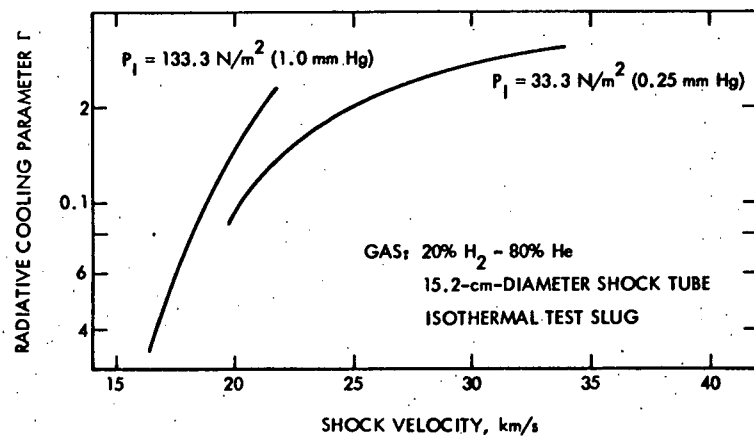


Fig. 8. Radiative cooling parameter for present experimental conditions

SYNOPTIC BACKUP DOCUMENT

This document is made publicly available through the NASA scientific and technical information system as a service to readers of the corresponding "Synoptic" which is scheduled for publication in the following (checked) technical journal of the American Institute of Aeronautics and Astronautics.

- ☒ AIAA Journal, October 1972
- ☐ Journal of Aircraft
- ☐ Journal of Spacecraft & Rockets
- ☐ Journal of Hydronautics

A Synoptic is a brief journal article that presents the key results of an investigation in text, tabular, and graphical form. It is neither a long abstract nor a condensation of a full length paper, but is written by the authors with the specific purpose of presenting essential information in an easily assimilated manner. It is editorially and technically reviewed for publication just as is any manuscript submission. The author must, however, also submit a full backup paper to aid the editors and reviewers in their evaluation of the synoptic. The backup paper, which may be an original manuscript or a research report, is not required to conform to AIAA manuscript rules.

For the benefit of readers of the Synoptic who may wish to refer to this backup document, it is made available in this microfiche (or facsimile) form without editorial or makeup changes.